PRAMANA
— journal of
physics

Vol. 54, No. 4
April 2000
pp. 573–587

Electromagnetic signals of quark gluon plasma

BIKASH SINHA
Variable Energy Cyclotron Centre, 1/AF Bidhannagar, Calcutta 700 064, India
Saha Institute of Nuclear Physics, 1/AF Bidhannagar, Calcutta 700 064, India

Abstract. Successive equilibration of quark degrees of freedom and its effects on electromagnetic signals of quark gluon plasma are discussed. The effects of the variation of vector meson masses and decay widths on photon production from hot strongly interacting matter formed after Pb + Pb and S + Au collisions at CERN SPS energies are considered. It has been shown that the present photon spectra measured by WA80 and WA98 Collaborations can not distinguish between the formation of quark matter and hadronic matter in the initial state.

Keywords. Fokker–Planck equation; vector mesons; photons.

PACS Nos 25.75.+r; 12.40.Yx; 13.85.Qk

1. Introduction

It is expected that two nuclei colliding at ultra-relativistic energies ($\sim$ 200 GeV/nucleon or more) may lead to hadronic matter go through a phase transition to its fundamental constituents, quarks and gluons, usually referred to as quark gluon plasma (QGP). Somewhat analogously, the universe, as per conventional wisdom should have consisted of quarks, gluons, leptons and photons, a microsecond after the Big Bang. The experience and wisdom, expected from nucleus–nucleus collisions in the laboratory are anticipated to facilitate our understanding of the quark-hadron phase transition although, I do not think I shall have time to discuss this rather fascinating topic. Indeed what possible footprints of that primordial epoch can be traced in today's cosmos is one of the interesting and intriguing questions (figure 1).

We focus [1] on electromagnetic signals in the laboratory experiments, photons in particular. One found that using the simplest possible thermal model of a first order phase transition there is a hint of the existence of the QGP, although the limits of the thermal photon data necessarily imply that a confident prediction is not possible yet [2]. With raw data of thermal photons coming out of lead–lead experiment at CERN [3] the scenario looks promising although a lot more work needs to be done to come to a definitive conclusion. Similarly, the 'mysterious' bump in the dilepton data of CERES and HELIOS do not seem to get explained that easily, QGP or otherwise [4].

Clearly, an understanding of the nature of the phase transition still remains an open question. Our lattice colleagues [5] tell us that for a pure SU(N) gauge the phase transition is second order for $N = 2$ and for $N = 3$, a first order phase transition takes

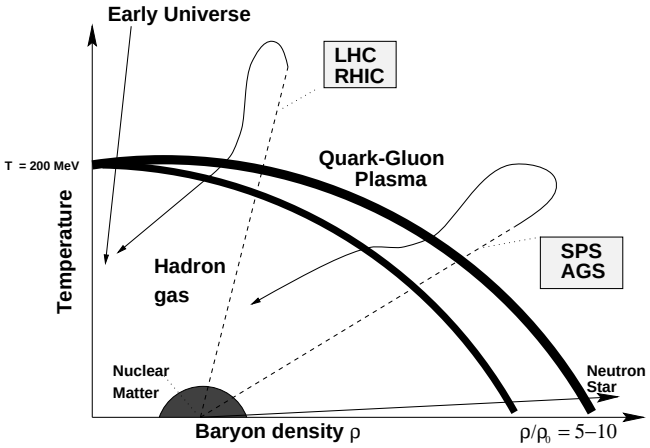

Figure 1. QCD phase diagram.

place. Introducing the fermions, the quarks, say u, d and s the scenario changes. For $N_f \geq 3$, the phase transition is of first order, but, continuous for $N_f = 2$. Using the non-equilibrium statistical mechanics and QCD it can be shown that thermal equilibrium is a possibility, however, chemical equilibrium is probably not acheived.

Indeed at initial time, whatever that is ($\tau \sim 1$ fm) it is unlikely that a pure QGP is formed, whereas a mixture of quark bubbles with hot hadronic matter is perhaps a more realistic possibility. The initial and boundary conditions which drive the space time evolution of the system is another area of intense discussion. Bjorken's simple scaling law [6] is certainly not valid, transverse expansion is a reality.

Our energetic friends [7] who deal with Parton cascade model (PCM) seem to have considerable insight on just these questions. There is now a real possibility that we can build simple models based on the distilled wisdom of the cascade crusaders.

In this paper, I will focus in these following areas: (1) the issue of successive thermal and chemical equilibrium scenarios and (2) a detailed study of photon emission from hot hadronic matter.

2. Approach to equilibrium

The primary motivation to study the non-equilibrium evolution of the quark–gluon system is driven from the fact that the characteristic time scales for the partonic processes are of the order of the lifetime of the *putative* QGP. Even if the system achieves thermodynamic equilibrium at some point of time, the study of the pre-equilibrium aspects is important to evaluate in the sense that the pollutants from this era may affect the kinematical domains where one looks for the signals of QGP. QGP diagnostics rely quite heavily on the phase space densities and distributions of quarks and gluons. To what extent equilibrium is achieved should obviously affect these signals.

To this end, the mechanisms governing the approach to thermalization in the quark–gluon system have been a very topical issue of late [7,8].

The central theme of our approach is to exploit the well-known result [9] that gg cross-section is considerably larger than qg or qq cross-sections, primarily because of the colour factor of gluons. It is therefore reasonable to expect that the gluons would thermalize among themselves appreciably earlier than the whole system of quarks, antiquarks, and gluons. The proper time τ_g at which the gluons equilibrate is thus considerably less [10] than the overall equilibration time τ_0; the value of τ_0 was proposed to be of the order of 1 fm/c by Bjorken [6] some time ago.

The gluons carry about 50% of the momentum and sea quarks only a tiny fraction. Thus, in very high energy collisions (RHIC or LHC energies), *if we confine our attention to the central rapidity region*, it is quite natural that from τ_g onwards, the equilibrated gluons may provide a thermal heat bath for the sea quarks (antiquarks). This picture is further justified by the fact that the sea quark (antiquark) density is very low compared to that of the gluons in this region [11]. Thus we are left with a system where a relatively small mixture of non-equilibrium degrees of freedom (quarks and antiquarks) interact with some equilibrated degree of freedom (the 'gluonic' bath); such processes are known to give rise to Brownian motion which is governed by the Fokker–Planck (FP) equation. QCD being asymptotically free, hard collisions involving large momentum transfers are suppressed compared to soft interactions and in our picture, thermalization in the quark–gluon system proceeds through many such soft collisions. The FP equation describes, semi-classically, the evolution of the many body quark–gluon system in a kinetic theory framework. The system under consideration is highly relativistic and presumably at high temperatures. Therefore, account of production and annihilation of $q\bar{q}$ pairs in the gluonic heat bath must be taken. The relativistic FP equation with these effects can be written as (see ref. [12] for derivation)

$$\frac{\partial f}{\partial t} - \frac{\partial}{\partial p_z}\left(\frac{a_p p_z f}{\sqrt{p_z^2 + m_T^2}}\right) - D_F \frac{\partial^2 f}{\partial p_z^2} = -\frac{f - f_{\rm eq}}{\tau_{\rm relax}}, \tag{1}$$

where $f_{\rm eq}$ is the equilibrium distribution and $\tau_{\rm relax}$ is the relaxation time estimated from the reactions $gg \leftrightarrow q\bar{q}$ and $g \leftrightarrow q\bar{q}$, m_T is the transverse mass ($= \sqrt{p_T^2 + m_{\rm eff}^2}$). $m_{\rm eff}$ is the effective mass defined as $m_{\rm eff} = \sqrt{m_{\rm current}^2 + m_{\rm thermal}^2}$, $m_{\rm current}$ is the current quark mass ($= 10$ MeV for u and d quarks) and $m_{\rm thermal}$ is the thermal mass: $m_{\rm thermal} = \sqrt{g_s^2 T^2/6}$, g_s is the strong coupling constant. In a chemically non-equilibrated scenario, the thermal mass is replaced by $m_{\rm thermal}^2 = (1 + r_q/2) g_s^2 T^2/9$ [13], where r_q is the ratio of equilibrium to non-equilibrium density. We have seen [14] that the effect of such a change on thermal mass has negligible effects on the final results.

It should be noted that the reactions $g\,g \leftrightarrow g\,g\,g\ldots$ etc. do not appear explicitly as the gluons have been assumed to be thermalized so that their density is determined from the temperature of the bath. Also, the thermal mass of the gluons is an essential ingredient; otherwise the reaction $g \leftrightarrow q\,\bar{q}$ would be forbidden.

2.1 *Cooling of the gluonic heat bath*

The gluonic heat bath is cooling due to expansion and the rate of cooling is determined by the relativistic hydrodynamics. The bulk properties of the system, e.g. the cooling law etc., are governed by the equilibrated degrees of freedom. In our case the cooling is given by the Bjorken's scaling law with appropriate modification due to quark production through

thermal gluon fusion $gg \rightarrow q\bar{q}$ and thermal gluon decay $g \rightarrow q\bar{q}$. We have obtained the cooling law [14] by solving the hydrodynamic equation which is parametrised as $T = \alpha/\tau^{\beta}$ where $\alpha = 0.4077$, $\beta = 0.355$ at LHC and $\alpha = 0.33$, $\beta = 0.352$ at RHIC energies respectively. The cooling rate in Bjorken model ($\beta = 1/3$) is slower compared to the present case where the production of quarks cost some energy.

2.2 *Solution of the Fokker–Planck equation*

We solve the FP equation with the following initial and boundary conditions for a quark species j

$$f_j(p_z, \tau) \overset{\tau \rightarrow \tau_g}{\longrightarrow} \Delta_j \delta(p_z) \tag{2}$$

and

$$f_j(p_z, \tau) \overset{|p_z| \rightarrow \infty}{\longrightarrow} 0. \tag{3}$$

The parameter Δ_j is determined from the initial density of the partons. $\delta(p_z)$ is a rather good approximation of the low x structure function [15]. We should also mention here that the final outcome of the model is insensitive to the functional form of the initial distribution function – a typical characteristic of the Markovian process.

It is important to mention here that the final outcome depends on the value of Δ_i. There is a lack of consensus about the initial value of the quark density. We take the initial values of quark densities from HIJING [16]. The phase-space density of quark is larger in case of parton cascade model [7] and also in the work of Shuryak [11]. In this sense our work corresponds to a conservative situation. The data from RHIC and LHC should make a distinction among various models.

As mentioned earlier, in the system under study the quark density changes with proper time due to two mechanisms. The expansion dynamics (flow) dilutes the density and on the other hand, the creation of quarks in the relativistic heat bath enhances the quark density. The gluon density decreases due to expansion only. We calculate the ratio of the width of the distribution in non-equilibrium and equilibrium situations, i.e. $\langle p_z^2 \rangle^{\text{non-eq}} / \langle p_z^2 \rangle^{\text{eq}}$. The advantage of calculating the ratio is that the expansion effects will get cancelled to some extent, though the cooling in the equilibrium and non-equilibrium scenario is different as has been mentioned before.

In figure 2 we plot these ratios as a function of the proper time τ. At RHIC (LHC) the initial thermalisation time, τ_g for the gluons is 0.3 fm/c (0.25 fm/c), the temperature $T_g(\tau_g)$ is 500 MeV (660 MeV) and the initial quark density $n_{u/d}$ is 0.7 fm^{-3} (2.8 fm^{-3}). At RHIC energy (figure 2a) we observe that the ratio D saturates to a value ~ 1, at a proper time $\tau \sim 3$ fm/c, well before the temperature of the system reaches to T_c (~ 160 MeV). In figure 2b we plot D for LHC energies; the thermal equilibration is complete within the proper time ~ 2 fm/c.

We evaluate the density of quarks in the non-equilibrium scenario by integrating the distribution function $f(p_z, \tau)G(p_T)$ over its momentum. The non-equilibrium density n_q has an explicit dependence on τ and an implicit dependence on τ through $T(\tau)$. But the equilibrium density $n_{\text{eq}}(T)$ has only an implicit dependence on τ through $T(\tau)$. The ratio

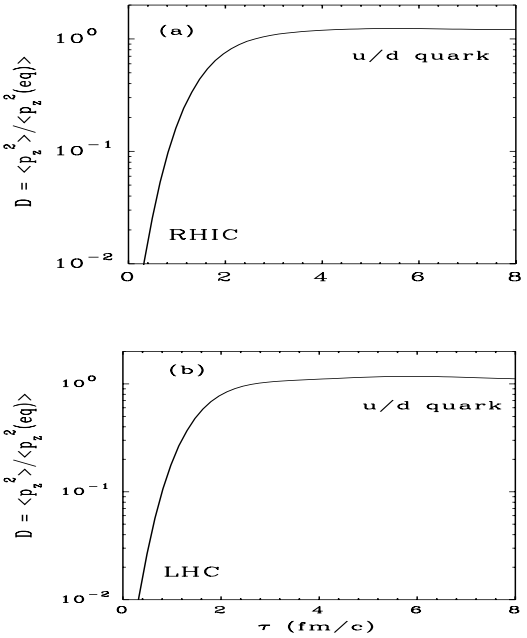

Figure 2. Ratio of the width of the distribution in non-equilibrium and equilibrium situations are plotted as a function of τ for RHIC and LHC.

$r_q = n(\tau)/n_{\rm eq}(T(\tau))$ thus assumes an *universal* feature, since the implicit time dependence gets eliminated. The time dependence of the ratio r_q can then be used as a ready marker for chemical equilibrium; the time at which the explicit time dependence of r_q vanishes, simultaneously with $r_q \to 1$, corresponds to the time for chemical equilibration for the flavour q. We observe from figure 3 that r_q neither saturates nor approaches the value unity before the temperature of the system reaches the value T_c (160 MeV). Therefore, we conclude that the chemical equilibrium is not achieved in the quark gluon system, although thermal (kinetic) equilibrium is. To show the sensitivity of the evolution of r_q on the initial quark density we show, in figure 3, the result of our calculations [14] obtained by taking initial quark density from the structure functions [10,15]. For the sake of completeness we also show the cooling law in figure 3, where $q\bar{q}$ production has been taken into account.

We have analysed the approach to thermal and chemical equilibrium in a quark gluon system within the framework of a semi-classical, physically transparent model. A fundamental consequence of this picture is that while thermal (kinetic) equilibrium is probable, chemical equilibrium is not, even for LHC energies. Even the kinetic equilibrium is achieved through a succession of time scales.

3. Photons from hot hadronic matter

Whether a QCD phase transition takes place or not, photons can be used as a probe to study the properties of hadrons in hot/dense medium. In a phase transition scenario, apart

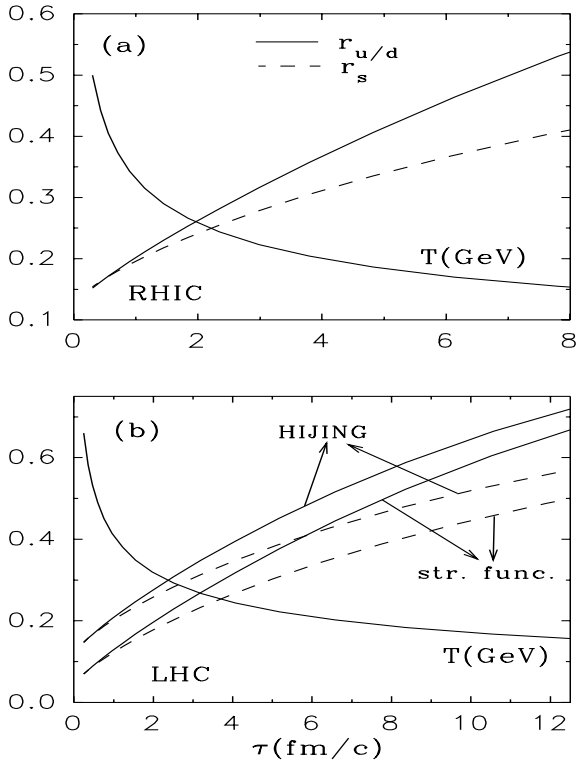

Figure 3. Plot of r_q as a function of τ.

from the QGP, photons are also produced from the thermalised hadronic gas, formed after the phase transition (see ref. [17] for details). Substantial contributions to the total photon yield also come from the initial hard collision of partons in the high momentum regime, and from hadronic decays ($\pi^0 \rightarrow \gamma\gamma, \eta \rightarrow \gamma\gamma$ etc.) in the low momentum zone. The hard QCD photons can be well understood through perturbative QCD and the decay photons can be reconstructed by invariant mass analysis. Thus, to extract photon signals from QGP it is essential to estimate the photon rates from various hadronic reactions and vector meson decays which is a challenging task, indeed. The temperature of the hadronic phase lies between 150–200 MeV. Therefore the finite temperature corrections to the hadronic properties and their consequences on photon spectra are very important.

For our purpose we model the hadronic gas as consisting of π, ρ, ω and η. First we consider the reactions $\pi\,\pi \rightarrow \rho\gamma$, $\pi\,\rho \rightarrow \pi\gamma$ and the decay $\rho \rightarrow \pi\pi\gamma$. We estimate the differential cross-section for photon production from the above processes taking into account the finite width of the rho meson (see ref. [18,19] for details.) The relevant vertices are obtained from the following Lagrangian:

$$\mathcal{L} = -g_{\rho\pi\pi}\vec{\rho}^{\mu} \cdot (\vec{\pi} \times \partial_{\mu}\vec{\pi}) - eJ^{\mu}A_{\mu} + \frac{e}{2}F^{\mu\nu}\,(\vec{\rho}_{\mu} \times \vec{\rho}_{\nu})_3, \tag{4}$$

where $F_{\mu\nu} = \partial_{\mu}A_{\nu} - \partial_{\nu}A_{\mu}$, is the Maxwell field tensor and J^{μ} is the hadronic part of the

electromagnetic current given by

$$J^{\mu} = (\vec{\rho}_{\nu} \times \vec{B}^{\nu\mu})_3 + (\vec{\pi} \times (\partial^{\mu}\vec{\pi} + g_{\rho\pi\pi}\vec{\pi} \times \vec{\rho}^{\mu}))_3 \tag{5}$$

with $\vec{B}_{\mu\nu} = \partial_{\mu}\vec{\rho}_{\nu} - \partial_{\nu}\vec{\rho}_{\mu} - g_{\rho\pi\pi}(\vec{\rho}_{\mu} \times \vec{\rho}_{\nu})$, and the subscript 3 after the cross product indicates the relevant component in isospin space.

We have also considered the photon production due to the reactions $\pi\,\eta \rightarrow \pi\,\gamma$, $\pi\,\pi \rightarrow \eta\,\gamma$ and the decay $\omega \rightarrow \pi\,\gamma$ (see ref. [18,19] for details).

In the case of nuclear collisions, one is more interested in overall photon rates rather than the cross-sections. Using independent particle approximation of kinetic theory [20] we can write down the rate of photon production per unit volume at a temperature T as

$$E\frac{\mathrm{d}R}{\mathrm{d}^3p} = \frac{\mathcal{N}}{16(2\pi)^7 E}\int_{(m_1+m_2)^2}^{\infty}\mathrm{d}s\int_{t_{\min}}^{t_{\max}}\mathrm{d}t\,|\mathcal{M}|^2\int\mathrm{d}E_1 \times\int\mathrm{d}E_2\frac{f(E_1)\,f(E_2)\,[1+f(E_3)]}{\sqrt{aE_2^2+2bE_2+c}}. \tag{6}$$

where $\mathcal{M}$ is the invariant transition amplitude of photon production for the appropriate reaction channel, evaluated from the Lagrangians given by eq. (4). For the parameters a, b, c please refer to [18,19].

3.1 VNN *interaction*

To calculate the effective mass and decay widths we begin with the following VNN (vector–nucleon–nucleon) Lagrangian density:

$$\mathcal{L}_{VNN} = g_{VNN}\left(\bar{N}\gamma_{\mu}\tau^{a}NV_{a}^{\mu} - \frac{\kappa_V}{2M}\bar{N}\sigma_{\mu\nu}\tau^{a}N\partial^{\nu}V_{a}^{\mu}\right), \tag{7}$$

where $V_a^{\mu} = \{\omega^{\mu}, \vec{\rho}^{\mu}\}$, M is the free nucleon mass, N is the nucleon field and $\tau_a = \{1, \vec{\tau}\}$. The values of the coupling constants g_{VNN} and κ_V will be specified later. With the above Lagrangian we proceed to calculate the ρ-self energy.

$$\Pi_{\mu\nu} = -2ig_{VNN}^2\int\frac{\mathrm{d}^4p}{(2\pi)^4}K_{\mu\nu}(p,k), \tag{8}$$

with

$$K_{\mu\nu} = \frac{\mathrm{Tr}\,[\Gamma_{\mu}(k)\,(\not{p}+M^*)\Gamma_{\nu}(-k)\,(\not{p}-\not{k}+M^*)]}{(p^2-M^{*2})((p-k)^2-M^{*2})}. \tag{9}$$

The vertex $\Gamma_{\mu}(k)$ is calculated by using the Lagrangian of eq. (7) and is given by

$$\Gamma_{\mu}(k) = \gamma_{\mu} + \frac{i\kappa_V}{2M}\sigma_{\mu\alpha}k^{\alpha}. \tag{10}$$

Here M^* is the in-medium (effective) mass of the nucleon at finite temperature which we calculate using the mean-field theory (MFT) [21]. The value of M^* can be found by solving the following self-consistent equation:

$$M^* = M - \frac{4g_s^2}{m_s^2} \int \frac{\mathrm{d}^3\mathbf{p}}{(2\pi)^3} \frac{M^*}{(\mathbf{p}^2 + M^{*2})^{1/2}} \left[f_N(T) + f_{\bar{N}}(T) \right], \tag{11}$$

where $f_N(T)(f_{\bar{N}}(T))$ is the Fermi–Dirac distribution for the nucleon (antinucleon), m_s is mass of the neutral scalar meson (σ) field, and, the nucleon interacts via the exchange of isoscalar meson with coupling constant g_s. Since the exact solution of the field equations in QHD is untenable, these are solved in mean field approximation. In a mean field approximation one replaces the field operators by their ground state expectation values which are classical quantities; this renders the field equations exactly solvable.

The vacuum part of the ρ-self energy arises due to its interaction with the nucleons in the Dirac sea. This is calculated using dimensional regularization scheme.

In a hot system of particles, there is a thermal distribution of real particles (on shell) which can participate in the absorption and emission process in addition to the exchange of virtual particles. The interaction of the rho with the onshell nucleons, present in the thermal bath contributes to the medium dependent part of the ρ-self energy. This is calculated from eq. (8) using imaginary time formalism as,

$$\begin{aligned} \mathrm{Re}\Pi_{\mathrm{med}}(\omega, \mathbf{k} \to 0) = \frac{16 g_{VNN}^2}{\pi^2} \int \frac{p^2\, \mathrm{d}p}{\omega_p \left(\mathrm{e}^{\beta\,\omega_p} + 1\right)(4\omega_p^2 - \omega^2)} \\ \times \left[\frac{1}{3}(2p^2 + 3M^{*2}) - \omega^2 \left\{ M^* \left(\frac{\kappa_V}{2M} \right) \right.\right. \\ \left.\left. - \frac{1}{3} \left(\frac{\kappa_V}{2M} \right)^2 (p^2 + 3M^{*2}) \right\} \right], \end{aligned} \tag{12}$$

where, $\omega_p^2 = p^2 + M^{*2}$.

3.2 *Finite temperature properties*

In this section we present the results of our calculation of the effective masses and decay widths of vector mesons. In figure 4 we show the variation of the ratio of effective mass to free mass for hadrons as a function of temperature. For our calculations of ρ and ω mesons effective masses we have used the following values of the coupling constants and masses [22]: $\kappa_\rho = 6.1$, $g_{\rho NN}^2/4\pi = 0.55$, m_s= 550 MeV, $m_\rho = 770$ MeV, $M = 938$ MeV, $g_s^2/4\pi = 9.3$, $g_{\omega NN}^2/4\pi = 20$, and κ_ω = 0.

The variation of the in-medium decay width (Γ_ρ) of the rho meson with temperature is shown in figure 5. As discussed earlier, the effective mass of the rho decreases as a result of $N\bar{N}$ polarisation. This reduces the phase space available for the rho. Hence, we observe a rapid decrease in the rho meson width with temperature (solid line). However, the presence of pions in the medium would cause an enhancement of the decay width through induced emission. Thus when Bose enhancement (BE) of the pions is taken into account the rho decay width is seen to fall less rapidly (dashed line). For the sake of completeness, we also show the variation of rho width in the case where the rho mass changes due to $\pi\pi$ loop. In this case, since the rho mass increases (though only marginally), the width increases (dot-dashed line).

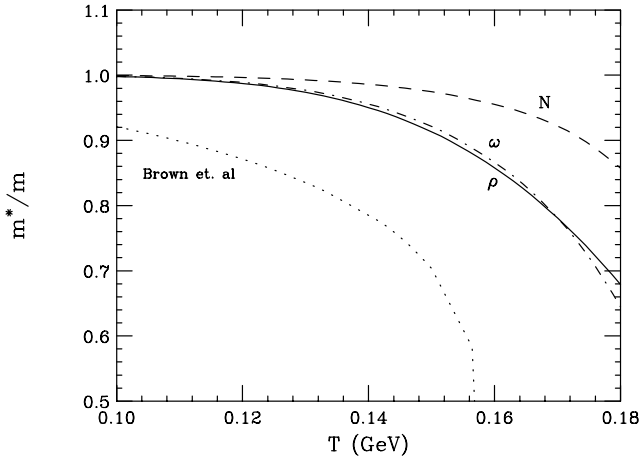

Figure 4. Ratio of effective mass to free space mass of hadrons as a function of temperature T. We do not observe any global scaling of masses as in [23].

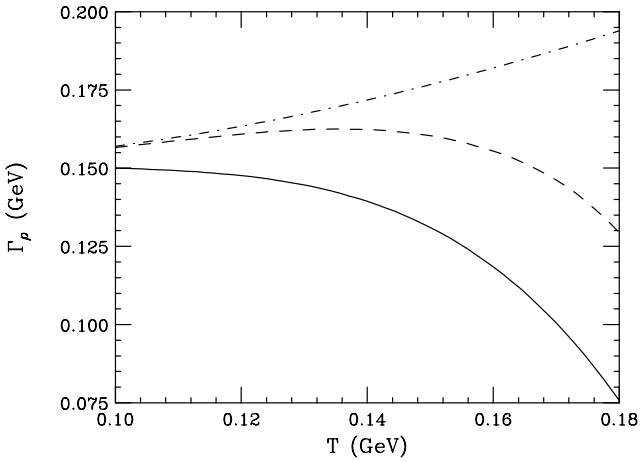

Figure 5. Rho decay width (Γ_ρ) as a function of temperature (T). Dashed and solid lines show calculations of rho width with effective mass due to nucleon loop, with and without BE. Dot dashed line represents the same but with effective mass due to pion loop.

3.3 *Photon emission rates*

In this section we present our results on photon emission rates from a hot hadronic gas. As discussed earlier, the variation of hadronic decay widths and masses will affect the photon spectra. The relevant reactions of photon production are $\pi\pi \rightarrow \rho\gamma, \pi\rho \rightarrow \pi\gamma, \pi\pi \rightarrow \eta\gamma$, and $\pi\eta \rightarrow \eta\gamma$ with all possible isospin combinations. Since the lifetimes of the rho and omega mesons are comparable to the strong interaction time scales, the decays

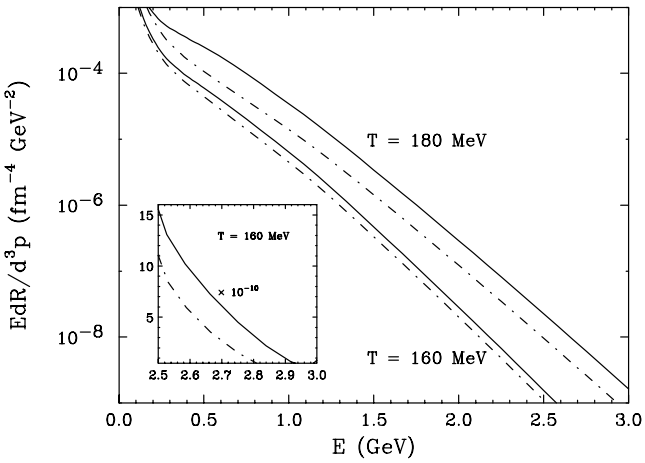

Figure 6. Total photon emission rate from hot hadronic matter as a function of photon energy at T=160, 180 MeV. The solid and dot-dashed lines show results with and without in-medium effects respectively. Inset: Total photon emission rate is plotted in linear scale as a function of photon energy in the kinematic window, $E_\gamma = 2.5$ to 3.0 GeV at $T = 180$ MeV.

$\rho \rightarrow \pi\pi\gamma$ and $\omega \rightarrow \pi^0\gamma$ are also included. The effect of finite resonance width of the rho meson in the photon production cross-sections has been taken into account through the propagator.

In figure 6 we display the total rate of emission of photons from hot hadronic gas including all hadronic reactions and decays of vector mesons. At $T = 180$ MeV, the photon emission rate with finite temperature effects is a factor of ~ 3 higher than the rate calculated without medium effects. At $T = 160$ MeV the medium effects are small compared to the previous case.

We have calculated the effective masses and decay widths of vector mesons propagating in a hot medium. We have seen that the mass of rho meson decreases substantially due to its interactions with nucleonic excitations and it increases only marginally ($\sim$ 10–15 MeV) due to $\rho - \pi$ interactions. The overall decrease in the effective mass is due to fluctuations in the Dirac sea of nucleons with mass M^* and the in-medium contribution decreases very little ($\sim$ 5–10 MeV) from its free space value. For ω mesons the in-medium contribution decreases by 80 MeV at $T = 180$ MeV but the Dirac sea effect is more prominent than the medium effect. The omega mass drops at $T = 180$ MeV by about 280 MeV from its free space value. Such changes in the properties of the vector mesons in hot and dense hadronic matter, as produced in heavy ion collisions, lead to the intriguing possibility of the opening of the decay channel $\omega \rightarrow \rho\pi$, for the omega meson, which is impossible in free space. This along with the channel $\omega\pi \rightarrow \pi\pi$ would result in a decrease in its effective life-time enabling it to decay within the hot zone and act as a chronometer in contradiction to the commonly held opinion and would have implications in determining the size of the region using pion interferometry. A new peak and a radically altered shape of the low invariant mass dilepton spectra appears due to different shift in the masses of ρ and ω mesons.

3.4 *Photon spectra from evolving matter*

The observed photon spectrum originating from an expanding QGP or hadronic matter is obtained by convoluting the static (fixed temperature) rate, as given by eq. (6), with expansion dynamics. Therefore, the second ingredient required for our calculations is the description of the system undergoing rapid expansion from its initial formation stage to the final freeze-out stage. In this work we use Bjorken-like [6] hydrodynamical model for the isentropic expansion of the matter in $(1+1)$ dimension. For the QGP sector we use simple bag model equation of state (EOS) with two flavour degrees of freedom. The temperature in the QGP phase evolves according to Bjorken scaling law $T^3\,\tau = T_i^3 \tau_i$.

In the hadronic phase we have to be more careful about the presence of heavier particles and their change in masses due to finite temperature effects. The hadronic phase consists of π, ρ, ω, η and a_1 mesons and nucleons. The nucleons and heavier mesons may play an important role in the EOS in a scenario where mass of the hadrons decreases with temperature.

The energy density and pressure for such a system of mesons and nucleons is given by

$$\epsilon_H = \sum_{i=\text{mesons}} \frac{g_i}{(2\pi)^3} \int \mathrm{d}^3p\, E_i\, f_{BE}(E_i, T) + \frac{g_N}{(2\pi)^3} \int \mathrm{d}^3p\, E_N\, f_{FD}(E_N, T) \tag{13}$$

and

$$P_H = \sum_{i=\text{mesons}} \frac{g_i}{(2\pi)^3} \int \mathrm{d}^3p \frac{p^2}{3\,E_i} f_{BE}(E_i, T) + \frac{g_N}{(2\pi)^3} \int \mathrm{d}^3p \frac{p^2}{3\,E_N} f_{FD}(E_N, T), \tag{14}$$

where the sum is over all the mesons under consideration and N stands for nucleons and $E_i = \sqrt{p^2 + m_i^2}$. The entropy density is given by

$$s_H = \frac{\epsilon_H + P_H}{T} \equiv 4a_{\text{eff}}(T)\, T^3 = 4\frac{\pi^2}{90} g_{\text{eff}}(m^*(T), T) T^3, \tag{15}$$

where g_{eff} is the effective statistical degeneracy.

Thus, we can visualise the finite mass of the hadrons having an effective degeneracy $g_{\text{eff}}(m^*(T), T)$. The variation of temperature from its initial value T_i to final value T_f (freeze-out temperature) with proper time (τ) is governed by the entropy conservation

$$s(T)\tau = s(T_i)\tau_i. \tag{16}$$

The initial temperature of the system is obtained by solving the following equation self consistently

$$\frac{\mathrm{d}N_\pi}{\mathrm{d}y} = \frac{45\zeta(3)}{2\pi^4} \pi\, R_A^2\, 4a_{\text{eff}} T_i^3 \tau_i, \tag{17}$$

where $\mathrm{d}N_\pi/\mathrm{d}y$ is the total pion multiplicity, R_A is the radius of the system, τ_i is the initial thermalisation time and $a_{\rm eff} = (\pi^2/90)\, g_{\rm eff}(m^*(T_i), T_i)$. The change in the expansion dynamics as well as the value of the initial temperature due to medium effects enters the calculation of the photon emission rate through the effective statistical degeneracy.

Let us consider Pb + Pb collisions at CERN SPS energies. If we assume that the matter is formed in the QGP phase with two flavours (u and d), then $g_k = 37$. Taking $\mathrm{d}N_\pi/\mathrm{d}y = 600$ as measured by the NA49 Collaboration [24] for Pb + Pb collisions, we obtain $T_i = 180$ MeV for $\tau_i = 1$ fm/c. The system takes a time $\tau_Q = T_i^3\tau_i/T_c^3$ to achieve the critical temperature of phase transition (T_c=160 MeV in our case). In a first order phase transition scenario the system remains in the mixed phase up to a time $\tau_H = r\,\tau_Q$, i.e. T remains at T_c for an interval $\tau_H - \tau_Q$, where r is the ratio of the statistical degeneracy in QGP to hadronic phase. At τ_H the system is fully converted to hadronic matter and remains in this phase up to a proper time τ_f. We have taken $T_f = 130$ MeV in our calculations.

In figure 7 we demonstrate the variation of temperature with proper time for different initial conditions. The dotted line indicates the scenario where QGP is formed initially at $T_i = 180$ MeV and cools down according to Bjorken law up to a temperature T_c at which a phase transition takes place; it remains constant at T_c up to a time $\tau_H = 8.4$ fm/c after which the temperature decreases as $T = 0.241/\tau^{0.19}$ to a temperature T_f. If the system is considered to be formed in the hadronic phase the initial temperature is obtained as $T_i = 230$ MeV (270 MeV) when in-medium effects on the hadronic masses are taken into account (ignored), the corresponding cooling laws are $T = 0.230/\tau^{0.169}$ ($T = 0.266/\tau^{0.2157}$) are displayed in figure 7 by solid and dashed lines respectively. The above parametrizations of the cooling law in the hadronic phase have been obtained by solving eq. (16) self consistently.

Obtaining the finite temperature effects on hadronic properties and the cooling law we are ready to evaluate the photon spectra from a $(1+1)$ dimensionally expanding system.

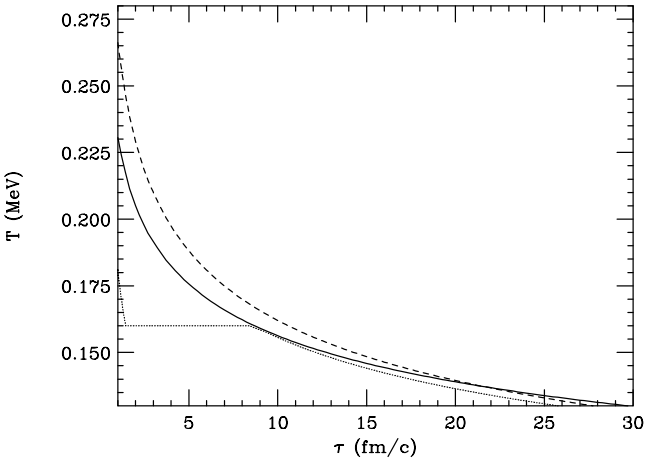

Figure 7. Variation of temperature with proper time. The dotted line indicates the cooling law in a first order phase transition scenario. The solid (dashed) line represents temperature variation in a 'hadronic scenario' with (without) medium effects on the hadronic masses.

The transverse momentum distribution of photons in a first order phase transition scenario is given by,

$$E\frac{\mathrm{d}N}{\mathrm{d}^3p} = \pi R_A^2 \int \Bigg[\left(E\frac{\mathrm{d}R}{\mathrm{d}^3p}\right)_{\mathrm{QGP}} \Theta(\epsilon - \epsilon_Q) + \Bigg[\left(E\frac{\mathrm{d}R}{\mathrm{d}^3p}\right)_{\mathrm{QGP}} \frac{\epsilon - \epsilon_H}{\epsilon_Q - \epsilon_H} + \left(E\frac{\mathrm{d}R}{\mathrm{d}^3p}\right)_{H} \frac{\epsilon_Q - \epsilon}{\epsilon_Q - \epsilon_H} \Bigg] \Theta(\epsilon_Q - \epsilon)\Theta(\epsilon - \epsilon_H) + \left(E\frac{\mathrm{d}R}{\mathrm{d}^3p}\right)_{H} \Theta(\epsilon_H - \epsilon) \Bigg] \tau \, \mathrm{d}\tau \, \mathrm{d}\eta, \tag{18}$$

where ϵ_Q (ϵ_H) is the energy density in the QGP (hadronic) phase at T_c, η is the space time rapidity, R_A is the radius of the nuclei and Θ functions are introduced to get the contribution from individual phases.

In figure 8 we compare our results of transverse momentum distribution of photons with the preliminary results of WA98 Collaboration [25]. The experimental data represents the photon spectra from Pb + Pb collisions at 158 GeV per nucleon at CERN SPS energies. The transverse momentum distribution of photons originating from the 'hadronic scenario' (matter formed in the hadronic phase) with (solid line) and without (short-dash line) medium modifications of vector mesons outshine the photons from the 'QGP scenario' (matter formed in the QGP phase, indicated by long-dashed line) for the entire range

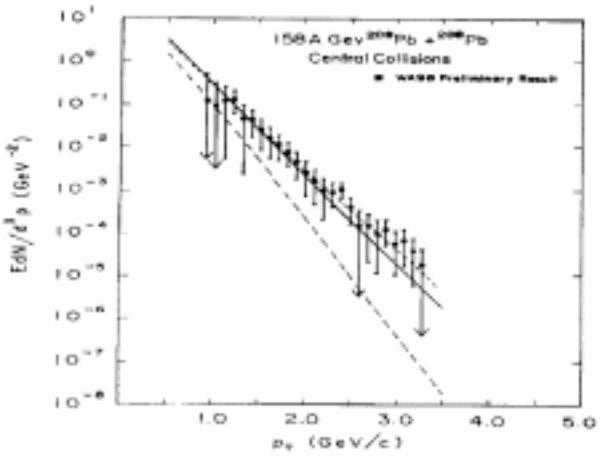

Figure 8. Total thermal photon yield in Pb + Pb central collisions at 158 GeV per nucleon at CERN SPS. The long-dash line shows the results when the system is formed in the QGP phase with initial temperature $T_i = 180$ MeV at $\tau_i = 1$ fm/c. The critical temperature for phase transition is taken as 160 MeV. The solid (short-dash) line indicates photon spectra when hadronic matter formed in the initial state at $T_i = 230$ MeV ($T_i = 270$ MeV) at $\tau_i = 1$ fm/c with (without) medium effects on hadronic masses and decay widths.

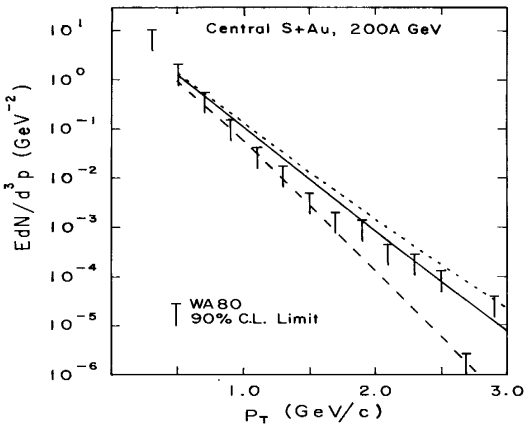

Figure 9. Total thermal photon yield in S + Au central collisions at 200 GeV per nucleon at CERN SPS. The long-dash line shows the results when the system is formed in the QGP phase with initial temperature $T_i = 190$ MeV at $\tau_i = 1.2$ fm/c. The critical temperature for phase transition is taken as 160 MeV. The solid (short-dash) line indicates photon spectra when hadronic matter formed in the initial state at $T_i = 230$ MeV ($T_i = 270$ MeV) at $\tau_i = 1.2$ fm/c with (without) medium effects on hadronic masses and decay widths.

of p_T. Although photons from 'hadronic scenario' with medium effects on vector mesons shine less bright than those from without medium effects for $p_T > 2$ GeV, it is not possible to distinguish clearly between one or the other on the basis of the experimental data.

In figure 9 we compare thermal photon spectra with the upper bound of WA80 Collaboration [26]. The experimental data stands for S + Au collisions at 200 GeV per nucleon at SPS. In this case the pion multiplicity, $\mathrm{d}N_\pi/\mathrm{d}y = 225$. Our calculation shows that maximum number of photons originate from the 'hadronic scenario' when the medium effects on vector mesons are ignored. For such a scenario the photon spectra has just crossed the upper bound of the WA80 data and more likely such a scenario is not realised in these collisions. Photons from 'hadronic scenario' with medium modifications of vector meson properties outshine those from the 'QGP scenario' for the entire p_T range. Considering the experimental uncertainty, no definitive conclusion can be drawn in favour of any particular scenario.

We have compared the experimental data on photon spectra from Pb + Pb and S + Au collisions at 158 GeV and 200 GeV per nucleon respectively with different initial conditions. In case of Pb + Pb collisions photons from hadronic scenario dominates over the photons from QGP scenario for the entire p_T domain. But in the hadronic scenario the photon spectra evaluated with and without in-medium properties of vector mesons describe these data reasonably well. Hence the transverse photon spectra at present do not allow us to decide between an in-medium dropping mass and a free mass scenario. For S + Au collisions the photon spectra evaluated with free masses seems to exceed the experimental upper limit. However, the photon spectra obtained by assuming hadronic matter (with in-medium effects or otherwise) in the initial state outshines the spectra evaluated with first

order phase transition scenario. Considering the experimental uncertainty, it is not possible to state, which one, between the two is compatible with the data. Experimental data with better statistics could possibly distinguish among various scenarios.

Acknowledgment

It is a great pleasure to thank J Alam, P Roy, S Sarkar and S Raha for their collaboration in the work reported here.

References

[1] B Sinha, in *Relativistic Aspects of Nuclear Collisions* edited by T Kodama *et al* (World Scientific, Singapore, 1996)
[2] D K Srivastava and B Sinha, *Phys. Rev. Lett.* **73**, 2421 (1994)
[3] B Wyslouch, in *Quark Matter'97*, Tsukuba, Japan
[4] D K Srivastava, B Sinha and C Gale, *Phys. Rev.* **C53**, R567 (1994)
[5] A Ukawa, in *Quark Matter'97*, Tsukuba, Japan
[6] J D Bjorken, *Phys. Rev.* **D27**, 140 (1993)
[7] K Geiger, *Phys. Rep.* **258**, 237 (1995)
[8] X N Wang, *Phys. Rep.* **280**, 287 (1997)
[9] R Cutler and D Sivers, *Phys. Rev.* **D17**, 196 (1978)
[10] E Shuryak, *Phys. Rev. Lett.* **68**, 3270 (1992)
[11] E Shuryak and L Xiong, *Phys. Rev. Lett.* **70**, 2241 (1993)
[12] P Roy, J Alam, S Sarkar, B Sinha and S Raha, *Nucl. Phys.* **A624**, 687 (1997)
[13] C T Traxler and M H Thoma, *Phys. Rev.* **C53**, 1348 (1996)
[14] J Alam, P Roy, S Sarkar, S Raha and B Sinha, *Int. J. Mod. Phys.* **A12**, 5151 (1997)
[15] M Glück, E Reya and A Vogt, *Z. Phys.* **C48**, 471 (1990)
[16] T S Biró, E van Doorn, B Müller, M H Thoma and X N Wang, *Phys. Rev.* **C48**, 1275 (1993)
[17] J Alam, S Raha and B Sinha, *Phys. Rep.* **273**, 243 (1996)
[18] S Sarkar, J Alam, P Roy, A Dutt-Mazumder, B Dutta-Roy and B Sinha, *Nucl. Phys.* **A634**, 206 (1998)
[19] P Roy, S Sarkar, J Alam and B Sinha, *Nucl. Phys.* **A653**, 277 (1999) nucl-th/9803052
[20] C Gale and J I Kapusta, *Phys. Rev.* **C35**, 2107 (1987)
[21] B D Serot and J D Walecka, *Advances in Nuclear Physics* (Plenum Press, New York, 1986) vol. 16
[22] R Machleidt, K Holinde and Ch Elster, *Phys. Rep.* **149**, 1 (1987)
[23] G E Brown and M Rho, *Phys. Rev. Lett.* **66**, 2720 (1991)
[24] P G Jones *et al*, *Nucl. Phys.* **A610**, 188c (1996)
[25] V Manko, *Int. Nucl. Phys. Conf.* (*INPC-98*), August '98, Paris, France
[26] R Albrecht *et al*, *Phys. Rev. Lett.* **76**, 3506 (1996)